

Robust-Load Frequency Controller Design For Iraqi National Super Grid System

Dr. Rashid H. Al-Rubayi *

Lokman H. Hassan Al-Sharafany

Received on: 1/9/2002

Accepted on: 8/4/2007

Abstract

This work is intended to design a new robust load-frequency controller for Iraqi National Super Grid System with uncertain parameters. Riccati equation approach to the stabilization of uncertain system is proposed. Robust controller that ensures stability of the closed-loop system for all admissible structured uncertainties is designed. 'Matching conditions' and Lyapunov stability theory are used to implement a robust stabilizing controller. Participation factor is used to address the interaction between the state variables and the modes in the power system. This property is used to choose weighting matrix of the state variables (Q). A linear, time, invariant mathematical model is derived for Iraqi National Super Grid System consisting of six generating stations with various types of turbines. The proposed approach is applied to this system and simulation program is built to evaluate its effectiveness.

(Uncertainty)

(Riccati)

(Uncertain systems)

Lyapunov (Matching conditions)

(Participation factor)

Weighting matrix

* Dept of Electrical and Electronic Eng, Univ of Tech, Iraq

LIST OF SYMBOLS

$A_{(n \times n)}$	System matrix		
$\Delta A(t)$	Uncertain system matrix		
ACE_i	Area control error of area i		
B_i	Frequency bias parameter for area i p.u. MW/Hz		
$B_{(n \times m)}$	input matrix		
$\Delta B(t)$	Uncertain input matrix		
			or gate travel
$C_{(r \times n)}$	Output matrix	$P_{tie,i}$	Tie-line power flow(positive out of area i), p.u. MW
D	Area load-frequency characteristic p.u. MW/ Hz	$P_{(n \times n)}$	Positive-definite symmetric matrix solution of Riccati equation
ΔE	Frequency and tie-line power deviation in bias setting of area i	PF	Participation factor
f	System frequency, Hz	ΔP_R	Governor gate position signal deviation in hydro unit or mechanical power deviation during steam reheat in reheat steam unit
$G(r(t))$	Continuous time matrix function	$Q_{(n \times n)}$	Symmetric positive semi-definite weighting matrix of state variable
H	Inertia constant, sec	$R_{(m \times m)}$	Symmetric positive-definite weighting matrix of control variable
$H(s(t))$	Continuous time matrix function	R_i	Governor speed regulation parameters, Hz / p.u. MW
$I_{(n \times n)}$	Identity matrix	T_{pi}	Generator time constant of area i, sec
K_{pi}	Generator gain constant of area i, Hz / p.u. MW	T_{pv}	Pilot valve time constant, sec
K_r	Reheat coefficient	T_1, T_2, T_3	General time constants for speed-governor, sec
K_i	Area control error integrator gain of area i	T_g	Time constant of thermal governor, sec
$K_{(m \times n)}$	Constant gain matrix		
LBP	Lower bound of parameters		
NP	Nominal parameters		
P_d	Area real load, MW		
$\Delta P_{d(m \times 1)}$	Disturbance vector		
P_g	Turbine output power, MW		
P_{max}, P_{min}	Power limits imposed by valve		

T_R	Dashpot time constant of hydro- governor, sec
T_r	Reheat time constant, sec
T_t	Turbine time constant of thermal area, sec
T_w	Water starting time, sec
T_{ij}^*	Synchronizing coefficient of tie-line p.u. MW
$U_{(m \times 1)}$	Input vector
UBP	Upper bound of parameters
$V(X(t))$	Lyapunov function
v_{ji}	Right eigenvector
w_{ji}	Left eigenvector
$X_{(n \times 1)}$	State-vector
$Y_{(r \times 1)}$	Output vector
δ	Power angle, rad., deg.
$\Gamma_{(n \times m)}$	Disturbance matrix
$\Delta\Gamma(t)$	Uncertain disturbance matrix
Δ	Deviation from initial value of a variable
$\alpha, \varepsilon_1, \eta, \sigma$	Positive constant
σ^*	Optimal value of σ
λ_i	I-th eigenvalue

1- Introduction

The primary objective of an electrical power system is to generate and deliver power as economically and reliably as possible and maintain balanced sinusoidal voltages with virtually constant magnitude and frequency.

It is known that the change in real power affects mainly the system frequency, while reactive power is less sensitive to changes in frequency and is mainly dependent on changes in voltage magnitude. Thus, real and reactive powers are controlled separately.

The load-frequency control (LFC) controls the real power and frequency and the automatic voltage regulator (AVR)

regulates the reactive power and voltage magnitude.

LFC or called automatic generation control (AGC) is very important item in power system operation and control for supplying sufficient and reliable electric power with good quality.

Different theories and techniques adopted by the researchers to study the load-frequency control are illustrated in the following:

Refs.[1-3], applied classical control theory to design controller for multi-area power system. Refs. [4-6], applied the optimal control theory to design the controller for multi-area power system. The design of the load-frequency controller using classical control theory and optimal control theory as mentioned above are based on the nominal plant parameters. This controller does not guarantee the stability and the desired performance of the power system under parametric uncertainties.

Refs. [7, 8], applied the concept of variable-structure system (VSS) to the design of load-frequency controller for both single area and multi-area systems. This approach can greatly improve the transient performance of the system. When the VSS is operated in the so called sliding mode, the system response becomes insensitive to change in the plant parameters. Pan and Liaw, [9], proposed a load-frequency controller consisting of an adaptive controller in parallel with an integral controller which can restrict the magnitude and rate of change of the control signal in order to satisfy practical limitations.

Wang, Zhou, and Wen, [10], and Goshaidas Ray, A.N Prasad, and G.D Prasad, [11], applied robust control theory to design the robust controller for multi-area power systems, taking into account the uncertainty of the parameters, using

two different ways.

To design a load-frequency controller that achieves stability and desired performance of the multi-area interconnected power system, it is preferred to use robust controller taking into account the uncertainty of the parameters appearing due to mathematical modeling of the power systems.

As mentioned above studies have been carried out to design robust load frequency controller of power systems. However these approaches are applied to study LFC problem for simplified models, i.e., only two-area with non-reheat steam turbines have been considered. In the present work the robust controller is designed for multi-area model consisting of six generating units with different types of turbines.

2- A Basic Problem In Robust Control System Design

The uncertain system may be represented in state-space form by the following equations:

$$\begin{aligned} \dot{X}(t) &= [A + \Delta A(t)]X(t) + [B + \Delta B(t)]U(t) \\ &+ [\Gamma + \Delta \Gamma(t)]\Delta P_d(t) \\ Y(t) &= CX(t) \end{aligned} \quad (1)$$

$\Delta A(t)$, $\Delta B(t)$ and $\Delta \Gamma(t)$ are the associated continuous time uncertainty matrices with proper dimensions. Fig.1 depicts a block symbolic representation of Eqs. (1).

The actuating signal U is given as $U = -KX(t)$. Here K is a $(m \times n)$ constant feedback matrix.

It is readily seen that determining a robust linear stabilizing control is equivalent to determining the constant gain matrix K .

3- Robust Feedback Controller

Consider the linear uncertain system represented by the state equation

$$\dot{X}(t) = [A + \Delta A(t)]X(t) + [B + \Delta B(t)]U(t) \quad (2)$$

where $A(n \times n)$ and $B(n \times m)$ are the nominal system matrices and the pair (A, B) is completely controllable.

Assume the following matching conditions:

$$\begin{aligned} \Delta A(t) &= AG(r(t)) \\ \Delta B(t) &= AH(s(t)) \end{aligned} \quad (3)$$

where the $G(r(t))$ and $H(s(t))$ are continuous time matrix functions of $r(t)$ and $s(t)$, respectively which are time variant and within allowable bounding set [11].

The system in Eq. (2) is said to be matched if there exist $G(r(t))$ and $H(s(t))$ mentioned above [11, 12].

A robust stabilizing feedback control is given by:

$$U(t) = -KX(t) = -\sigma^* R^{-1} B^T P X(t) \quad (4)$$

where R is $(m \times m)$ symmetric positive definite weighting matrix, and η , ϵ_1 and σ are positive constants.

Q be any $(n \times n)$ given symmetric positive semi-definite weighting matrix and there exists an optimal $\sigma^* > 0$ such that for all values of σ larger than σ^* have a positive definite solution of the following Riccati equation:

$$\begin{aligned} A^T P + P A - 2 \sigma^* P B R^{-1} B^T P + \eta G^T(r(t)) \\ G(r(t)) + Q = [0] \end{aligned} \quad (5)$$

with

$$\sigma^* \left[\frac{I}{\varepsilon_1} + \varepsilon_1 A H(s(t)) R^{-1} B^T B R^{-1} H^T(s(t)) A^T \right] \geq \eta A^T A \quad (6)$$

And the closed-loop system matrix is asymptotically stable for all admissible uncertainty matrices $G(r(t))$ and $H(s(t))$ [11].

Note that the optimal value of σ can be computed as:

$$\frac{1}{\eta} \frac{\lambda_{\max}[A A^T]}{\lambda_{\min} \left[\frac{I}{\varepsilon_1} + \varepsilon_1 A H(s(t)) R^{-1} B^T B R^{-1} H^T(s(t)) A^T \right]} \quad (7)$$

where λ is eigenvalue of the matrix

In most cases, both Q and R are chosen as diagonal matrices.

The flowchart for determining the robust stabilizing control law is given in Fig. 2.

4- Participation Factors

The participation factor of the j -th variable in the i -th mode is defined as the product of the j -th's components of the right v_{ji} and left w_{ji} eigenvector corresponding to the i -th mode [13]

$$PF_{ji} = w_{ji} v_{ji} \quad (8)$$

The sensitivity of the eigenvalue λ_i with respect to a parameter q can be computed as [14]

$$\frac{\partial \lambda_i}{\partial q} = w_i^T \frac{\partial A(q)}{\partial q} v_i \quad (9)$$

If the parameter q is a diagonal entry of the state matrix A_{jj} , the eigenvalue sensitivity becomes the participation factor of the eigenvalue λ_i in the state variable X_j

$$\frac{\partial \lambda_i}{\partial A_{jj}} = w_{ji} v_{ji} = PF_{ji} \quad (10)$$

Hence, using the participation factor for identifying the state variables that have significant importance this property is employed to choose the weighting matrix of the state variables (Q).

5- Robust Performance

The final goal of robust control is to achieve the performance requirement on all members of the family of models (i.e. robust performance).

In this work the 'performance robustness' is considered as a difference in the shape of the

transient responses from the nominal response.

To demonstrate the performance robustness of the proposed controller, we define the following 'Norms' and absolute 'Sums' as [11].

$$\begin{aligned} Norm_{UBP} &= \left\{ \sum_{i=0}^k [X_{NP}(iT) - X_{UBP}(iT)]^2 \right\}^{\frac{1}{2}} \\ Norm_{LBP} &= \left\{ \sum_{i=0}^k [X_{NP}(iT) - X_{LBP}(iT)]^2 \right\}^{\frac{1}{2}} \\ Sum_{UBP} &= \sum_{i=0}^k |X_{NP}(iT) - X_{UBP}(iT)| \\ Sum_{LBP} &= \sum_{i=0}^k |X_{NP}(iT) - X_{LBP}(iT)| \end{aligned} \quad (11)$$

where $X_{NP}(iT)$, $X_{UBP}(iT)$ and $X_{LBP}(iT)$ represent the value of any state X at i -th instant of time, when the system parameters are at the nominal values, upper and lower bounds respectively.

The flowchart for determining the performance robustness of the proposed controller is given in Fig. 3.

6- Modelling Of Iraqi National Super Grid System

The Iraqi National Super Grid System consists of 19 bus bars and 29 transmission lines including the two lines connecting BABYL and QADISIYA. The two lines have been connected in 2001. Six generating stations with different types of turbines are connected to the grid. The configuration of the network is given in Ref. [15]. The network is reduced to a simplified form as shown in Fig. 4. The reduction is carried out by eliminating nodes to which only static elements are connected using Gauss reduction method. This configuration is obtained by reformulating the Y-bus matrix of order 19*19 to a new matrix of order 6*6 and from the power flow calculations the loads are distributed on each area.

Detailed block diagram representation of the Iraqi National Super Grid System for LFC is shown in Fig. 5. Each area is represented by the model for the governor and turbine, taking into consideration the limitation of the valve position and generator rating.

1- Area one

Station: Mosul Dam

$$\begin{aligned}\dot{X}_1 &= -\frac{1}{T_{p1}} X_1 + \frac{K_{p1}}{T_{p1}} X_2 - \frac{K_{p1}}{T_{p1}} X_5 - \frac{K_{p1}}{T_{p1}} \Delta P_{d1} \\ \dot{X}_2 &= \frac{2T_R}{R_1 T_1 T_2} X_1 - \frac{2}{T_w} X_2 + \left(\frac{2}{T_w} + \frac{2}{T_2}\right) X_3 \\ &\quad - \left(\frac{2}{T_2} - \frac{2T_R}{T_1 T_2}\right) X_4 + \frac{2T_R}{T_1 T_2} X_{31} - \frac{2T_R}{T_1 T_2} U_1 \\ \dot{X}_3 &= -\frac{T_R}{R_1 T_1 T_2} X_1 - \frac{1}{T_2} X_3 + \left(\frac{1}{T_2} - \frac{T_R}{T_1 T_2}\right) X_4 \\ &\quad - \frac{T_R}{T_1 T_2} X_{31} + \frac{T_R}{T_1 T_2} U_1 \\ \dot{X}_4 &= -\frac{1}{R_1 T_1} X_1 - \frac{1}{T_1} X_4 - \frac{1}{T_1} X_{31} + \frac{1}{T_1} U_1 \\ \dot{X}_{31} &= B_1 X_1 + X_5\end{aligned}\quad (12)$$

where

$$\begin{aligned}X_1 &= \Delta f_1; X_2 = \Delta P_{g1}; X_3 = \Delta X_{E1}; \\ X_4 &= \Delta P_{R1}; X_{31} = \Delta E_1\end{aligned}$$

2- Area two

Station: BAIJI

$$\begin{aligned}\dot{X}_6 &= -\frac{a_{12} K_{p2}}{T_{p2}} X_5 - \frac{1}{T_{p2}} X_6 + \frac{K_{p2}}{T_{p2}} X_7 - \frac{K_{p2}}{T_{p2}} X_{10} \\ &\quad - \frac{K_{p2}}{T_{p2}} X_{11} - \frac{K_{p2}}{T_{p2}} \Delta P_{d2} \\ \dot{X}_7 &= -\frac{1}{T_1} X_7 + \frac{1}{T_1} X_8 \\ \dot{X}_8 &= -\frac{1}{T_3} X_8 + \frac{1}{T_3} X_9 \\ \dot{X}_9 &= -\frac{1}{R_2 T_1} X_6 - \frac{1}{T_1} X_9 - \frac{1}{T_1} X_{32} + \frac{1}{T_1} U_2 \\ \dot{X}_{32} &= B_2 X_6 + a_{12} X_5 + X_{10} + X_{11}\end{aligned}\quad (13)$$

where

$$\begin{aligned}X_6 &= \Delta f_2; X_7 = \Delta P_{g2}; X_8 = \Delta X_{E2}; \\ X_9 &= \Delta P_{R2}; X_{32} = \Delta E_2\end{aligned}$$

3- Area three**Station: Qadisiya**

$$\begin{aligned}
\dot{X}_{12} &= -\frac{a_{23}K_{p3}}{T_{p3}}X_{10} - \frac{1}{T_{p3}}X_{12} + \frac{K_{p3}}{T_{p3}}X_{13} - \frac{K_{p3}}{T_{p3}}X_{16} \\
&\quad - \frac{K_{p3}}{T_{p3}}\Delta P_{d3} \\
\dot{X}_{13} &= \frac{2T_R}{R_3T_1T_2}X_{12} - \frac{2}{T_w}X_{13} + \left(\frac{2}{T_w} + \frac{2}{T_2}\right)X_{14} \\
&\quad - \left(\frac{2}{T_2} - \frac{2T_R}{T_1T_2}\right)X_{15} + \frac{2T_R}{T_1T_2}X_{33} - \frac{2T_R}{T_1T_2}U_3 \quad (14) \\
\dot{X}_{14} &= -\frac{T_R}{R_3T_1T_2}X_{12} - \frac{1}{T_2}X_{14} + \left(\frac{1}{T_2} - \frac{T_R}{T_1T_2}\right)X_{15} \\
&\quad - \frac{T_R}{T_1T_2}X_{33} + \frac{T_R}{T_1T_2}U_3 \\
\dot{X}_{15} &= -\frac{1}{R_3T_1}X_{12} - \frac{1}{T_1}X_{15} - \frac{1}{T_1}X_{33} + \frac{1}{T_1}U_3 \\
\dot{X}_{33} &= a_{23}X_{10} + B_3X_{12} + X_{16}
\end{aligned}$$

where

$$\begin{aligned}
X_{12} &= \Delta f_3, \quad X_{13} = \Delta P_{g3}, \quad X_{14} = \Delta X_{E3}, \\
X_{15} &= \Delta P_{R3} \text{ and } X_{33} = \Delta E_3
\end{aligned}$$

4- Area four**Station: Musiab**

$$\begin{aligned}
\dot{\Delta f}_{17} &= -\frac{a_{24}K_{p4}}{T_{p4}}X_{11} - \frac{a_{34}K_{p4}}{T_{p4}}X_{16} - \frac{1}{T_{p4}}X_{17} \\
&\quad + \frac{K_{p4}}{T_{p4}}X_{18} - \frac{K_{p4}}{T_{p4}}X_{21} - \frac{K_{p4}}{T_{p4}}\Delta P_{d4} \\
\dot{X}_{18} &= -\frac{1}{T_r}X_{18} + \left(\frac{1}{T_r} - \frac{K_t}{T_t}\right)X_{19} + \frac{K_t}{T_t}X_{20} \\
&\quad (15) \\
\dot{X}_{19} &= -\frac{1}{T_t}X_{19} + \frac{1}{T_t}X_{20} \\
\dot{X}_{20} &= \frac{1}{R_4T_3}X_{17} - \frac{1}{T_3}X_{20} - \frac{1}{T_3}X_{34} + \frac{1}{T_3}U_4 \\
\dot{X}_{34} &= a_{24}X_{11} + a_{34}X_{16} + B_4X_{17} + X_{21}
\end{aligned}$$

where

$$\begin{aligned}
X_{17} &= \Delta f_4; \quad X_{18} = \Delta P_{g4}; \quad X_{19} = \Delta P_{R4}; \\
X_{20} &= \Delta X_{E4}; \quad X_{34} = \Delta E_4
\end{aligned}$$

5- Area five**Station: Nasiriya**

$$\begin{aligned}
\dot{X}_{22} &= -\frac{a_{45}K_{p5}}{T_{p5}}X_{21} - \frac{1}{T_{p5}}X_{22} + \frac{K_{p5}}{T_{p5}}X_{23} \\
&\quad - \frac{K_{p5}}{T_{p5}}X_{26} - \frac{K_{p5}}{T_{p5}}\Delta P_{d5} \\
\dot{X}_{23} &= -\frac{1}{T_t}X_{23} + \frac{1}{T_t}X_{24} \\
&\quad (16) \\
\dot{X}_{24} &= -\frac{1}{T_3}X_{24} + \frac{1}{T_3}X_{25} \\
\dot{X}_{25} &= -\frac{1}{R_5T_1}X_{22} - \frac{1}{T_1}X_{25} - \frac{1}{T_1}X_{35} + \frac{1}{T_1}U_5 \\
\dot{X}_{35} &= a_{45}X_{21} + B_5X_{22} + X_{26}
\end{aligned}$$

Where

$$\begin{aligned}
X_{22} &= \Delta f_5; \quad X_{23} = \Delta P_{g5}; \quad X_{24} = \Delta X_{E5}; \\
X_{25} &= \Delta P_R; \quad X_{35} = \Delta E_5
\end{aligned}$$

6- Area Six**Station: Hartha**

$$\begin{aligned}
\dot{X}_{27} &= -\frac{a_{56}K_{p6}}{T_{p6}}X_{26} - \frac{1}{T_{p6}}X_{27} + \frac{K_{p6}}{T_{p6}}X_{28} \\
&\quad - \frac{K_{p6}}{T_{p6}}\Delta P_{d6} \\
\dot{X}_{28} &= -\frac{1}{T_t}X_{28} + \frac{1}{T_t}X_{29} \\
&\quad (17) \\
\dot{X}_{29} &= -\frac{1}{T_3}X_{29} + \frac{1}{T_3}X_{30} \\
\dot{X}_{30} &= -\frac{1}{R_6T_1}X_{27} - \frac{1}{T_1}X_{30} - \frac{1}{T_1}X_{36} + \frac{1}{T_1}U_6 \\
\dot{X}_{36} &= a_{56}X_{26} + B_6X_{27}
\end{aligned}$$

Where

$$X_{27} = \Delta f_6; X_{28} = \Delta P_{g6}; X_{29} = \Delta X_{E6};$$

$$X_{30} = \Delta P_{R6}; X_{36} = \Delta E_6$$

6- Tie-line model

$$\begin{aligned} \dot{X}_5 &= T_{12}^*(X_1 - X_6) \\ \dot{X}_{10} &= T_{23}^*(X_6 - X_{12}) \\ \dot{X}_{11} &= T_{24}^*(X_6 - X_{17}) \\ \dot{X}_{16} &= T_{34}^*(X_{12} - X_{17}) \\ \dot{X}_{21} &= T_{45}^*(X_{17} - X_{22}) \\ \dot{X}_{26} &= T_{56}^*(X_{22} - X_{27}) \end{aligned} \tag{18}$$

where

$$X_5 = \Delta P_{tie,1}; X_{10} = \Delta P_{tie,2};$$

$$X_{11} = \Delta P_{tie,3}; X_{16} = \Delta P_{tie,4};$$

$$X_{21} = \Delta P_{tie,5} \text{ and } X_{26} = \Delta P_{tie,6}$$

Eqs. (12), (13), (14), (15), (16), (17) and (18) can, upon rearrangement, be put in the form of nominal system matrices (A, B and Γ).

7- Simulation Results And Discution

Parameters of each area under study are given in Table 1 [15].

The nominal parameters, data and the range of the parameter variations of the power system under study is given in Appendix B [15].

Table 1 Parameters of the six areas.

Area No.	T _p , sec	K _p	δ ,deg
1	32.376	84.134	6.38
2	5.211	16.286	0.0
3	6.911	36.764	0.78
4	3.333	12.820	-4.92
5	18.598	48.945	-0.53
6	7.664	20.169	-2.61

The nominal system matrices (B ,A and Γ) are calculated by substituting the numerical values of the parameters and the initial conditions in the system state equations derived in previous section.

To study and analyze the effect of a load increase on the open-loop system (system without controller) response, a 10 % step load change is assumed to take place at HARTHA power station.

The frequency, tie-line power and generator output power responses are obtained by solving the linear system differential equations using the Runge-Kutta fourth order approximation for a step length 0.08 second. The simulation results with upper and lower bound parameter variations are presented in Fig. 6. Figs. 6-a and 6-b show the frequency deviations in area one and area six respectively, Fig. 6-c shows the power deviation in the tie-line six and Fig. 5-d shows the generator output power deviation of area six.

From these figures it is clear that open-loop system with lower bound parameter variations is unstable and the system with nominal and upper bound parameter variations is stable but with high amount of oscillations in the frequency, tie-line power and generator output power deviations. Hence, the transient behavior of the system should be improved. To enhance the stability and desired performance the proposed approaches is applied on this system.

To compute robust feedback controller gains using proposed approach, the following initial data have been considered:

$$R = I_{16 \times 16}, \epsilon_1 = 0.01, \eta = 10,$$

$$X(0) = [0 \ 0 \ 0 \ 0 \ \dots \ 0]^T$$

The eigenvalues and their damping r

ratios of the system with nominal parameters are calculated and listed in Table 2.

For identifying the state variables that have significant importance, the participation factors are calculated as shown in Table 3.

From Table 2, it is clear that there is one critical eigenvalue (λ_{36}) and there are twelve poorly damped oscillation modes ($\lambda_1, \lambda_2, \lambda_3, \lambda_4, \lambda_5, \lambda_6, \lambda_7, \lambda_8, \lambda_9, \lambda_{10}, \lambda_{25}$ and λ_{26}).

Table 3 indicates that dominant eigenvalue λ_{36} is associated with state variables X_{10}, X_{11} and X_{16} ; eigenvalues (λ_1 and λ_2) are associated with state variables X_5, X_6, X_{10} and X_{12} ; eigenvalues (λ_3 and λ_4) are associated with state variables $X_{11}, X_{12}, X_{16}, X_{17}$ and X_{21} ; eigenvalues (λ_5 and λ_6) are associated with state variables $X_5, X_{12}, X_{22}, X_{26}$ and X_{27} ; eigenvalues (λ_7 and λ_8) are associated with state variables X_1, X_5, X_{17}, X_{26} and X_{27} ; eigenvalues (λ_9 and λ_{10}) are associated with state variables $X_1, X_{11}, X_{21}, X_{22}$ and X_{27} and eigenvalues (λ_{25} and λ_{26}) are associated with state variables $X_{18}, X_{22}, X_{23}, X_{28}, X_{35}$ and X_{36}

Mode No.	Eigenvalue λ	Damping ratio (%)
1	-0.0833 + j24.727	0.337
2	-0.0833 - j24.727	0.3.37
3	-0.1020 + j19.2487	0.530
4	-0.1020 - j19.2487	0.530
5	-0.0482 +	0.330
6	-0.0482 - j14.5975	0.330
7	-0.0606 +	0.499
8	-0.0606 - j12.1402	0.499
9	-0.0323 + j6.0929	0.531
10	-0.0323 - j6.0929	0.531
11	-10.3799	100
12	-9.9110	100
13	-9.9178	100
14	-8.4548 + j0.6472	99.7
15	-8.4548 - j0.6472	99.7
16	-8.4556	100
17	-8.4472	100
18	-3.0656	100
19	-2.7094	100
20	-2.6791	100
21	-0.8920 + j1.2220	59.0
22	-0.8920 - j1.2220	59.0
23	-1.3168	100
24	-1.1856	100
25	-0.0081 + j0.5246	1.55
26	-0.0081 - j0.5246	1.55
27	-0.3741 + j0.4284	65.8
28	-0.3741 - j0.4284	65.8
29	-0.3905	100
30	-0.0655 + j0.1871	33.1
31	-0.0655 - j0.1871	33.1
32	-0.0477 + j0.1510	30.1
33	-0.0477 - j0.1510	30.1
34	-0.0560 + j0.3727	14.9
35	-0.0560 - j0.3727	14.9
36	0.0000	100

so that the weighting matrix Q is chosen as :

Table 2 Eigenvalues and their damping ratios.

Table 3 Participation factors for each state variable associated with each mode.

Stat	λ_1	λ_2	λ_3	λ_4	λ_5	λ_6	λ_7	λ_8	λ_9	λ_{10}	λ_{25}	λ_{26}	λ_{36}
X ₁	0.01	0.01	0.00	0.00	0.06	0.06	0.13	0.13	0.15	0.15	0.07	0.07	0.00
X ₅	0.10	0.10	0.01	0.01	0.12	0.12	0.19	0.19	0.05	0.05	0.00	0.00	0.00
X ₆	0.29	0.29	0.01	0.01	0.04	0.04	0.01	0.01	0.04	0.04	0.02	0.02	0.00
X ₁₀	0.31	0.31	0.04	0.04	0.03	0.03	0.02	0.02	0.00	0.00	0.00	0.00	0.14
X ₁₁	0.06	0.06	0.13	0.13	0.01	0.01	0.03	0.03	0.13	0.13	0.00	0.00	0.22
X ₁₂	0.17	0.17	0.10	0.10	0.10	0.10	0.04	0.04	0.01	0.01	0.02	0.02	0.00
X ₁₆	0.01	0.01	0.10	0.10	0.02	0.02	0.00	0.00	0.03	0.03	0.00	0.00	0.62
X ₁₇	0.01	0.01	0.30	0.30	0.00	0.00	0.11	0.11	0.00	0.00	0.03	0.03	0.00
X ₁₈	0.00	0.00	0.00	0.00	0.00	0.00	0.00	0.00	0.00	0.00	0.11	0.11	0.00
X ₂₁	0.00	0.00	0.18	0.18	0.07	0.07	0.02	0.02	0.21	0.21	0.00	0.00	0.00
X ₂₂	0.00	0.00	0.06	0.06	0.16	0.16	0.03	0.03	0.12	0.12	0.11	0.11	0.00
X ₂₃	0.00	0.00	0.00	0.00	0.00	0.00	0.00	0.00	0.00	0.00	0.27	0.27	0.00
X ₂₆	0.00	0.00	0.02	0.02	0.21	0.21	0.20	0.20	0.05	0.05	0.00	0.00	0.00
X ₂₇	0.00	0.00	0.00	0.00	0.11	0.11	0.15	0.15	0.16	0.16	0.06	0.06	0.00
X ₂₈	0.00	0.00	0.00	0.00	0.00	0.00	0.00	0.00	0.00	0.00	0.15	0.15	0.00
X ₃₅	0.00	0.00	0.00	0.00	0.00	0.00	0.00	0.00	0.00	0.00	0.27	0.27	0.00
X ₃₆	0.00	0.00	0.00	0.00	0.00	0.00	0.00	0.00	0.00	0.00	0.15	0.15	0.00

Table 4 Performance robustness of the proposed controller.

Stat e	Norms		Sums	
	Norm UBP	Norm LBP	Sum UBP	Sum LBP
Δf_1	0.023	0.035	0.140	0.307
ΔP_{gl}	0.023	0.033	0.139	0.258

Stat	Norms		Sums	
$\Delta P_{tie,1}$	0.057	0.080	0.256	0.431
Δf_2	0.018	0.029	0.124	0.293
$\Delta P_{tie,2}$	0.028	0.036	0.133	0.227
$\Delta P_{tie,3}$	0.039	0.079	0.258	0.586
Δf_3	0.023	0.031	0.146	0.301
$\Delta P_{tie,4}$	0.015	0.029	0.099	0.211
Δf_4	0.020	0.030	0.138	0.288
$\Delta P_{tie,5}$	0.057	0.106	0.467	1.036

Stat	Norms		Sums	
Δf_5	0.019	0.031	0.134	0.304
$\Delta P_{tie,6}$	0.052	0.087	0.432	0.858
Δf_6	0.022	0.034	0.152	0.327
ΔP_{g6}	0.037	0.074	0.444	0.933

The time domain responses with upper and lower bound parameter variations of the controlled system is obtained and plotted in Figs. 7 to 9. These figures show the dynamic behavior of the system under controller action when subjected to 10 % step load change at HARTHA power station.

Table 5 Settling time of state variables.

State	Settling time, sec		
	Nominal parameter	Parameter perturbation	Parameter perturbation
		(upper limit)	(lower limit)
Δf_1	8	7	12
Δf_2	9	8	14
Δf_3	9	8	14
Δf_4	9	8	14
Δf_5	9	6	12
Δf_6	9	5	12

ΔP_{g1}	10	10	15
ΔP_{g6}	12	8	15
$\Delta P_{tie,1}$	8	8	10
$\Delta P_{tie,2}$	9	9	11
$\Delta P_{tie,3}$	8	8	14
$\Delta P_{tie,4}$	7	7	14
$\Delta P_{tie,5}$	8	8	14
$\Delta P_{tie,6}$	12	8	14

Fig. 7 shows the frequency responses of six generating areas. Fig. 8 show the tie-line power responses and Fig. 9 show

the generator output power responses of area one and area six.

Analysis of the results obtained reveals that the proposed controller guarantees the stability of the Iraqi National Super Grid System under parametric uncertainties.

The numerical results of the performance robustness are computed and listed in Table 4.

From Table 4 it is clear that the Norm of the deviation in each state variable is more less than the percentage values of parametric variations from their nominal values.

For example the Norm of the deviation in the $\Delta P_{tie,5}$ is 0.1066, which is the

maximum one among the values stated in the Table, is more less than the percentage values of parametric variations (30%).

Table 5 shows the settling time of the frequency, generator output power deviation in each area and the tie-line power deviation.

8- Conclusions

In this study, a new load-frequency controller for power systems with uncertainty of the parameters is suggested. This control scheme is developed based on centralized approach. Stability analysis of the proposed approach has been established based on ‘matching conditions’ and Lyapunov stability theory.

A linearized mathematical model is derived for Iraqi National Super Grid System. The system contains 36 state variables, for six generation areas having different types of turbines.

From this research, the following points can be drawn:

1. It is concluded that the dynamic response of the systems by the proposed robust controller ensures stability of the closed-loop system for all admissible structured uncertainties.
2. The proposed approach involves trial and error for choosing the weighting matrix Q to obtain a desired performance. However, it is observed that using participation factors to identify the state variables that have significant importance will reduce number of ‘trial and error’ processes.
3. Applying this approach on Iraqi National Super Grid System, the results show that the frequency and tie-line power deviation reach their steady state (zero deviation) in about 14 sec. This settling time is practically acceptable.
4. It may be noted that tuning parameters (ϵ_1 and η) play an important role to stabilize the uncertain systems.

Appendix

A - Time Constant

Area No.	$T_{1,s}$ ec	$T_{2, sec}$	$T_{3,s}$ ec	$T_{R,s}$ ec	T_w, sec	T_t, sec	T_r, sec	H, sec
1	48.7	0.513	--	5.0	1.0	--	--	9.6
2	0.2	0.0	0.1	--	--	0.25	--	8.0
3	48.7	0.513	--	5.0	1.0	--	--	4.7
4	0.0	0.0	0.1	--	--	0.25	6.0	6.5
5	0.1	0.0	0.12	--	--	7.0	--	9.5
6	0.1	0.0	0.12	--	--	7.0	--	9.5

B- The Range of Parameter Variations

Parameter	Area 1	Area 2	Area 3	Area 4	Area 5	Area 6
	Upper limit	Upper limit	Upper limit	Upper limit	Upper limit	Upper limit
$1/T_p$	0.046	0.285	0.216	0.450	0.080	0.195
K_p/T_p	3.9	4.687	7.978	5.769	3.945	3.945
T_R/RT_1T_2	0.15	--	0.15	--	--	--
$1/T_w$	1.3	--	1.3	--	--	--
$1/T_1$	0.026	6.50	0.026	--	13.0	13.0
$1/RT_1$	0.015	3.75	0.015	--	7.50	7.50
$1/T_2$	2.534	--	2.534	--	--	--
T_R/T_1T_2	0.260	--	0.260	--	--	--
$1/T_t$	--	5.20	--	5.20	0.185	0.185
$1/RT_3$	--	--	--	7.50	--	--
K_r/T_t	--	--	--	2.60	--	--
$1/T_r$	--	--	--	0.216	--	--
$1/T_3$	--	13.0	--	13.0	10.83	10.83

References

- [1] Elgerd O.I. and Fosha C.E., “**Optimum Megawatt-Frequency Control of Multi-area Electric Energy Systems**”, IEEE Trans. on PAS, Vol. PAS-89, No. 4, April 1970, PP. 556-563.
- [2] Tripathy S.C., Hope G.S. and Malik O.P., “**Optimization of Load-Frequency Control Parameters for Power Systems with Reheat Steam Turbines and Governor Dead band Nonlinearity**”, IEE Proc., Vol. 129, Pt. C. No. 1, Jan. 1982, PP. 10-16.
- [3] Nanda J. Kothari M.L. and Satsangi P.S., “**Automatic Generation Control of an Interconnected Hydro-thermal System in Continuous and Discrete Modes Considering Generation Rate Constraints**”, IEE Proc., Vol. 130, Pt. D, No. 1, Jan. 1983, PP. 17-27.
- [4] Fosha C.E. and Elgerd O.I., “**The Megawatt-Frequency Control problem: A New Approach Via Optimal Control Theory**”, IEEE Trans. on PAS, Vol. PAS-89, No. 4, April 1970, PP. 563-577.
- [5] Calovic M., “**Linear Regulator Design of a Load and Frequency Control**”, IEEE Trans. on PAS, Vol. PAS-91, Feb. 1972, PP. 2271-2285.
- [6] Malik O.P., Hope G.S., Tripathy S.C., and Mital, N., “**Decentralized Suboptimal Load-Frequency Control of a Hydro-Thermal Power System Using the State Variable Model**”, Electric Power Systems Research. 8, (1984/1985), PP. 237-247.
- [7] Chan, W.C. and Hsu, Y.Y., “**Automatic Generation control of Interconnected Power Systems Using Variable-Structure Controllers**”, IEE Proc., Vol. 128, Pt. C, No. 5, Sept. 1981, PP. 269-279.
- [8] Sivaramakrishnan A.Y., Hariharan M.V. and Srisailam M.C., “**Design of Variable-Structure Load-Frequency Controller Using Pole Assignment Technique**”, Int. J. Control, Vol. 40, No.
- [9] Pan C.T. and Liaw C.M., “**An Adaptive controller for Power Load-Frequency Control**”, IEEE Trans. on Power Systems, Vol. 4, No. 1, Feb. 1989, PP. 122-128.
- [10] Wang Y., Zhou R. and Wen C., “**Robust Load-Frequency Controller Design for Power Systems**”, IEE Proc., Vol. 4, Pt. C., No. 140, 1993, PP. 11-18.
- [11] Ray G., Prasad A.N. and Prasad G.D., “**A New Approach to the Design of Robust Load-Frequency Controller for Large Scale Power Systems**”, Electric Power Systems Research, Vol. 51, 1999, PP. 13-22.
- [12] Dorata P., “**Robust Control**”, IEEE Press, 1987.
- [13] Perez-Arriaga I.J., Verghese G.C. and Schweppe F.C., “**Selective Modal Analysis of Power System Oscillatory Instability**”, IEEE Trans. on Power Systems, Vol. 3, No. 2, May 1988, PP. 429-438.
- [14] Rouco L., “**Eigenvalue-Based Methods for Analysis and Control of Power System Oscillations**”, PE-547-PWRS-0-01, 1998.

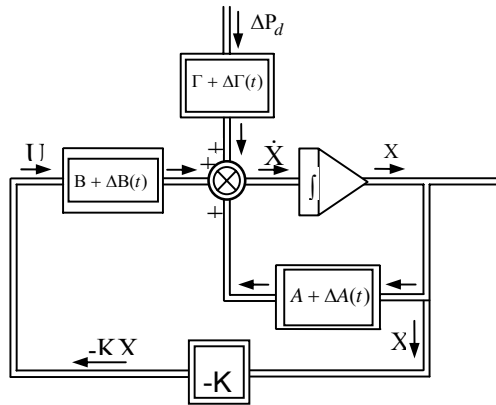


Fig. 1 Block diagram of controlled uncertain linear system

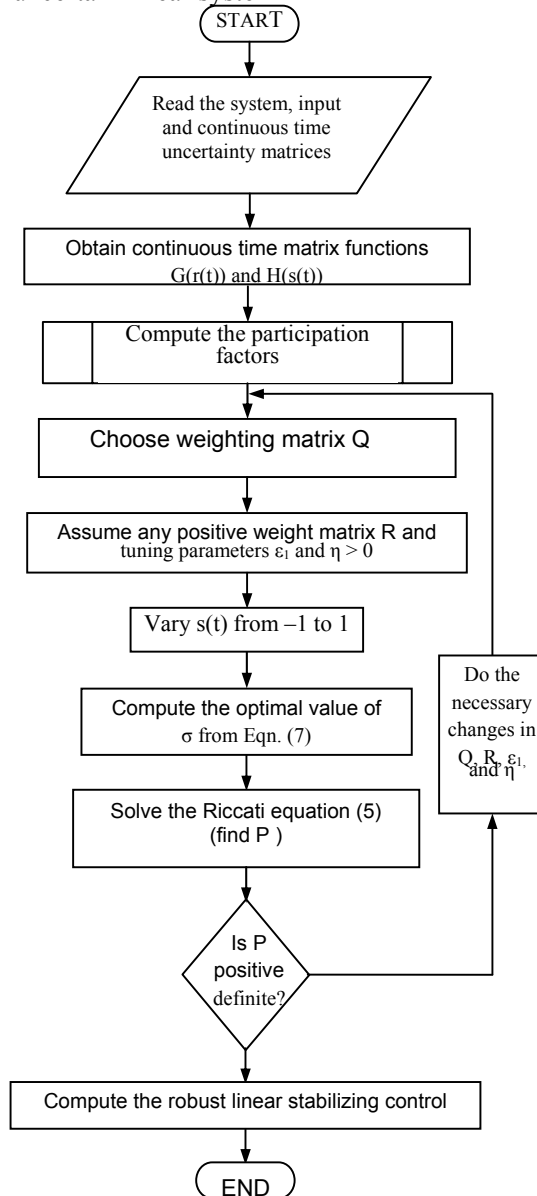


Fig. 2 Flowchart for designing robust stabilizing controller.

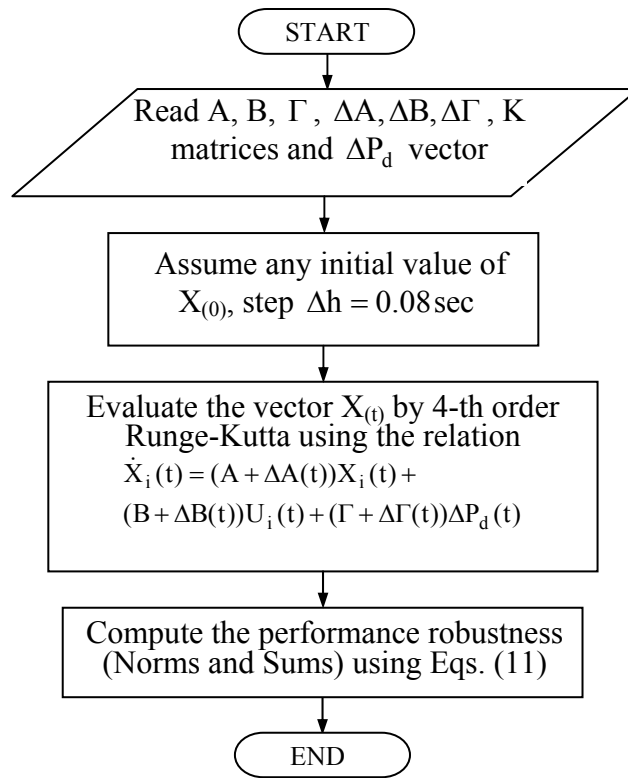


Fig. 3 Flowchart for determining the performance robustness of the controller.

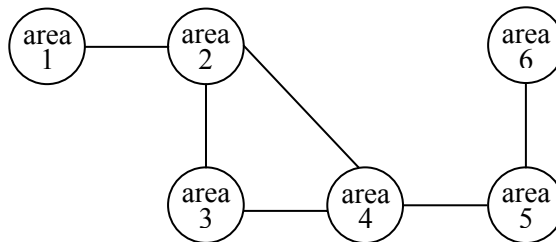


Fig. 4 General diagram of Iraqi National Super Grid System

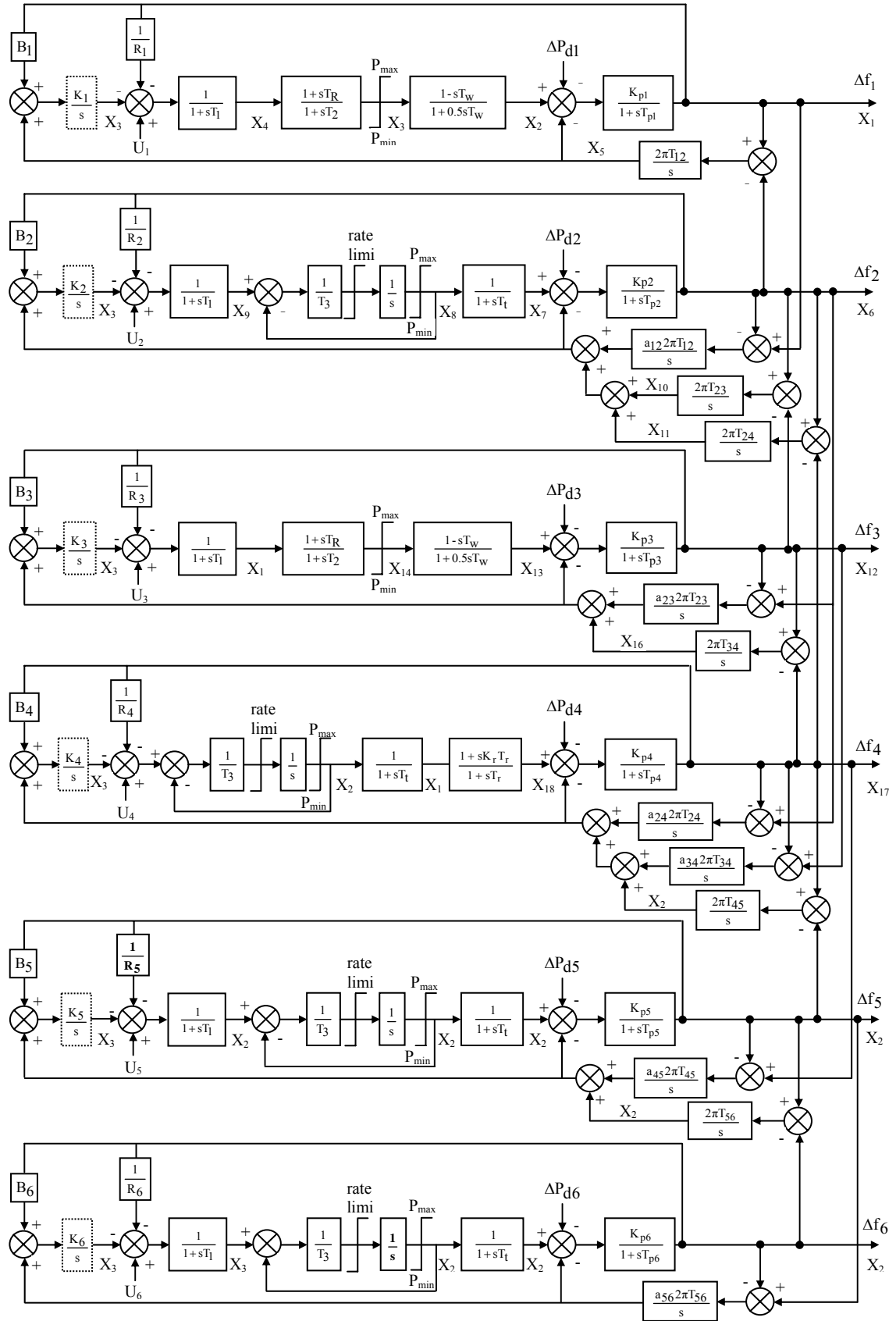
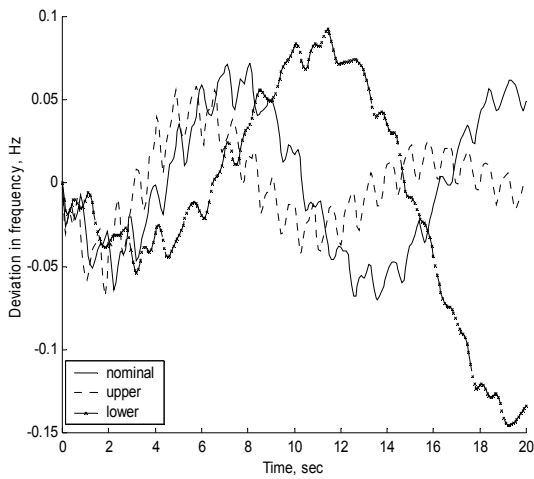
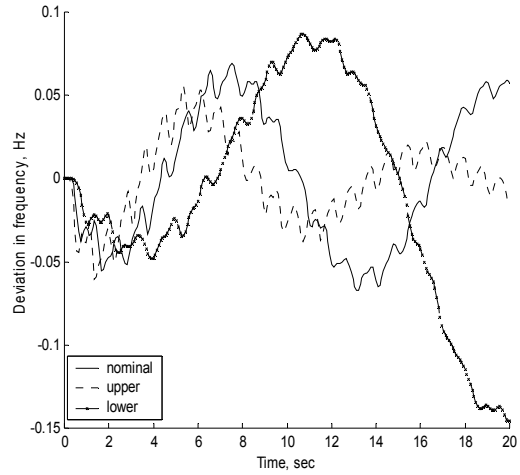


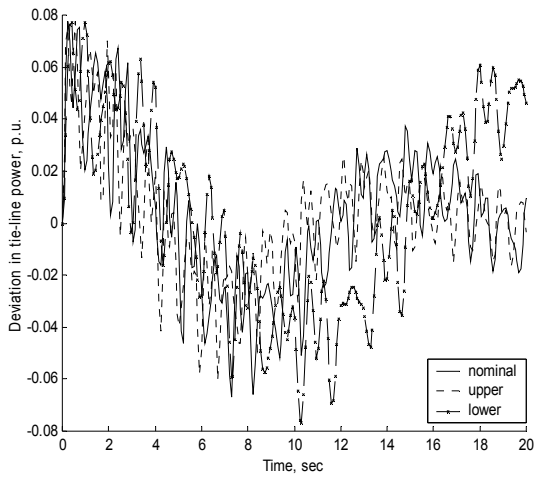
Fig. 5 Block diagram of Iraqi National Super Grid System for LFC.



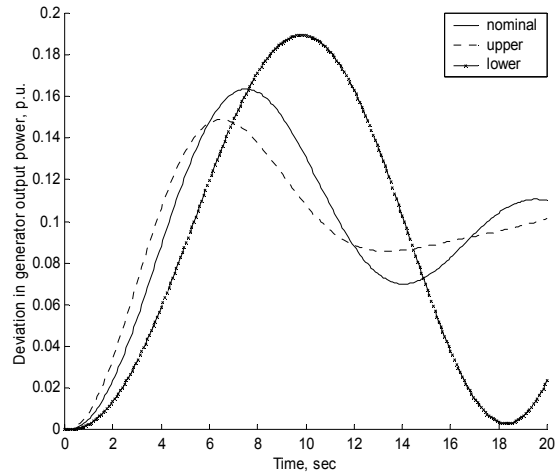
(a) Frequency response of area one (f_1).



(b) Frequency response of area six (f_6).

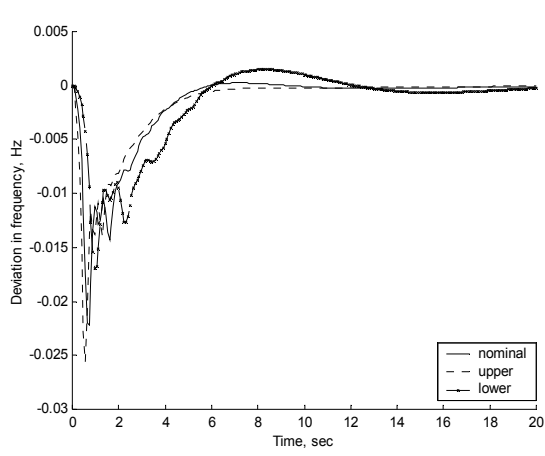


(c) Generator output power response of area six (P_{g6}).

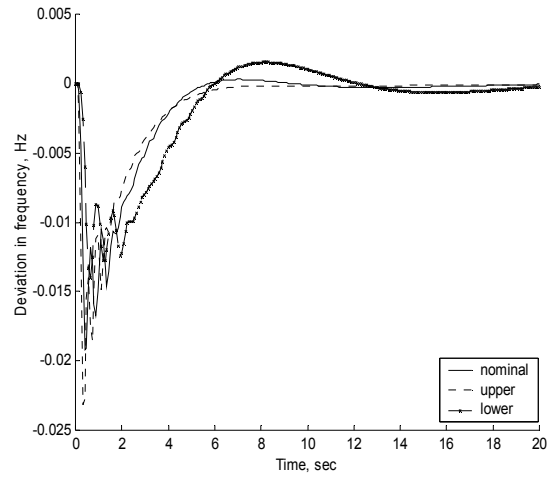


(d) Tie-line power response ($P_{tie,6}$).

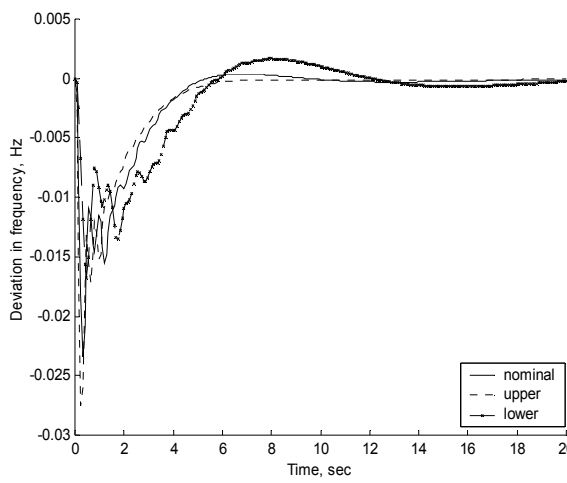
Fig. 6 System response for 10 % step load change in area six (HARTHA) without controller.



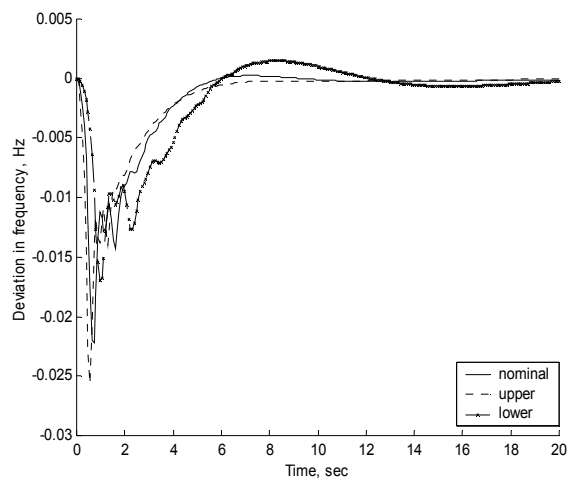
(a) Frequency response of area one (f_1).



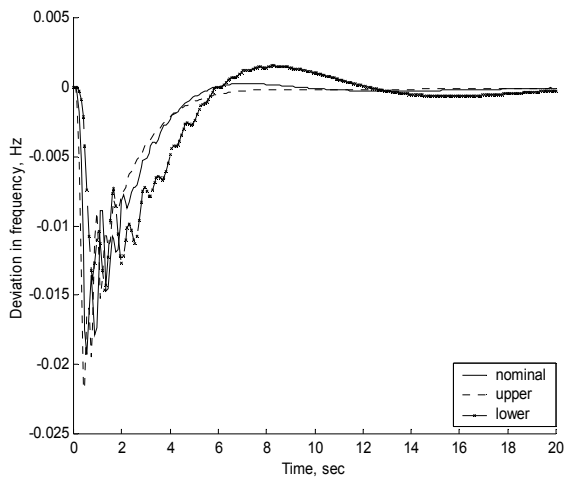
(d) Frequency response of area four (f_4).



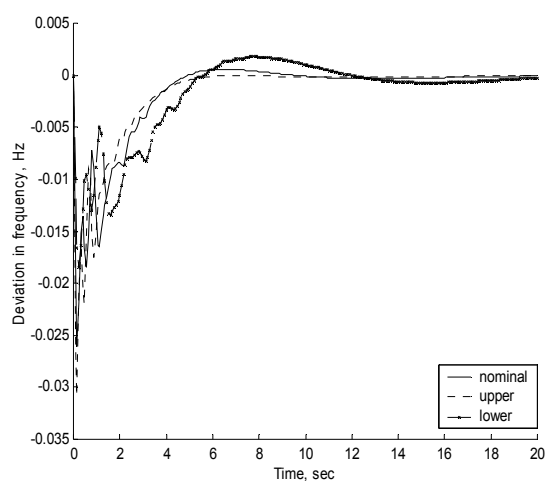
(b) Frequency response of area two (f_2).



(e) Frequency response of area five (f_5).



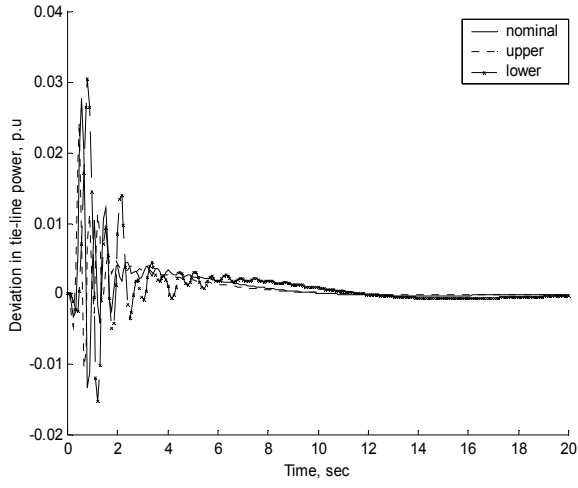
(c) Frequency response of area three (f_3).



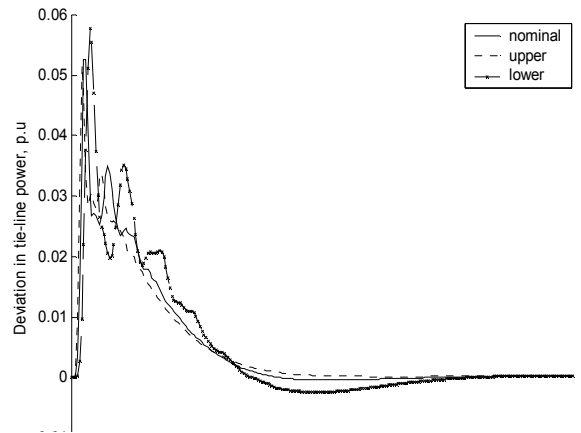
(f) Frequency response of area six (f_6).

Fig. 7 Tie-line power response for 10 % step load change in area six (HARTHA).

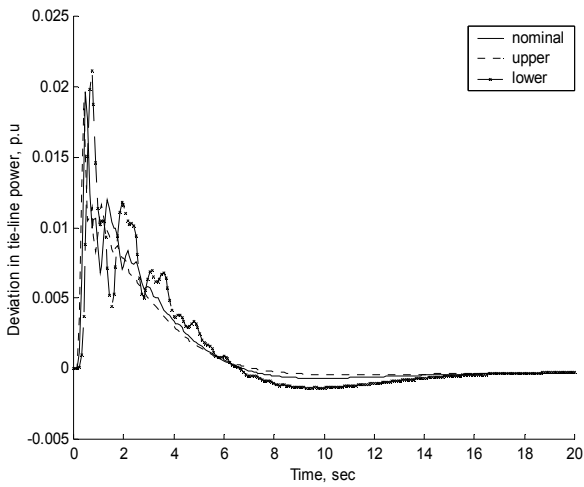
En;



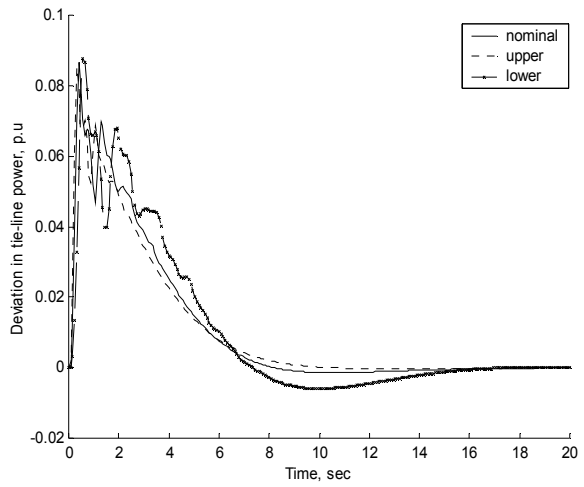
(a) Tie-line power response ($P_{tie,1}$).



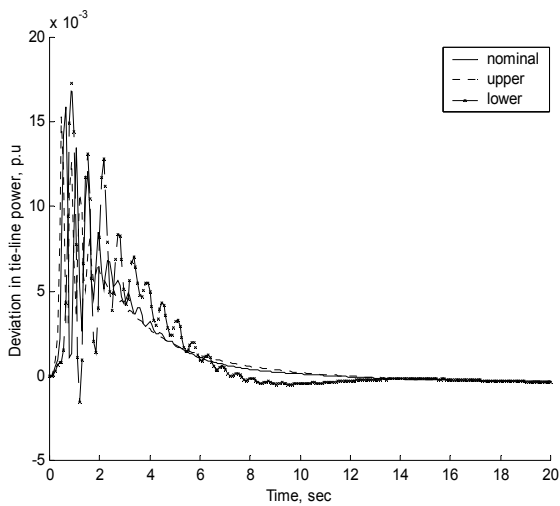
(d) Tie-line power response ($P_{tie,4}$).



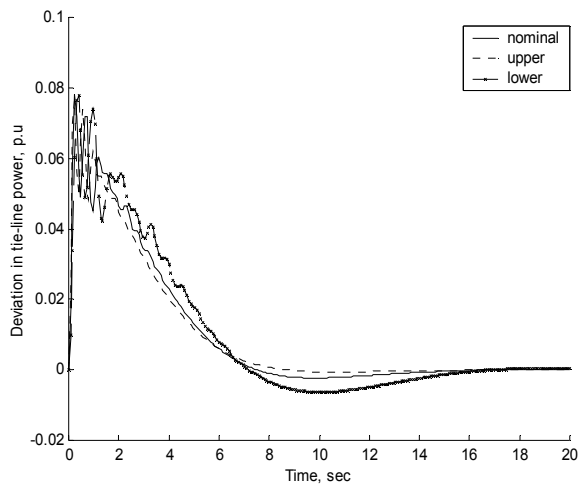
(b) Tie-line power response ($P_{tie,2}$).



(e) Tie-line power response ($P_{tie,5}$).

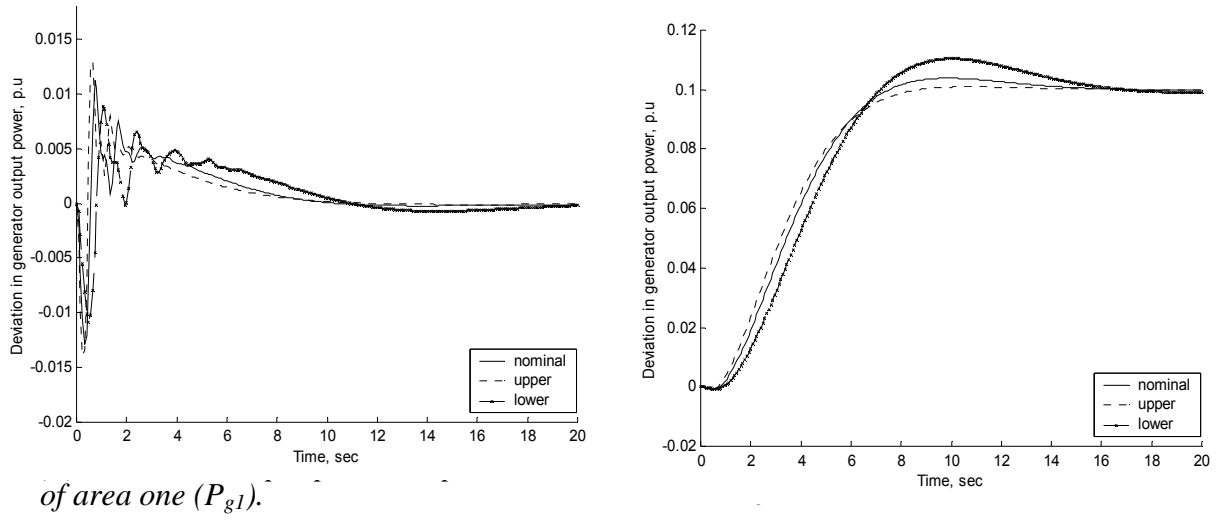


(c) Tie-line power response ($P_{tie,3}$).



(f) Tie-line power response ($P_{tie,6}$).

Fig. 8 Tie-line power response for 10 % step load change in area six (HARTHA).



of area one (P_{g1}).

Fig. 9 Generator output power response for 10 % step load change in area six (HARTHA).